Journal of The Electrochemical Society, **153** (8) G746-G749 (2006)
0013-4651/2006/153(8)/G746/4/$20.00 © The Electrochemical Society

Electrical Characterization and Surface Morphology of Optimized Ti/Al/Ti/Au Ohmic Contacts for AlGaN/GaN HEMTs

J. A. Bardwell,*,z S. Haffouz, H. Tang, and R. Wang

Institute for Microstructural Sciences, National Research Council, Ottawa, Ontario, Canada K1A 0R6

Low-resistance ohmic contacts to high-electron-mobility transistors (HEMTs) are essential to ensure optimal device performance. Besides low contact resistance (<1 Ω mm), good surface morphology and edge acuity are also desirable. We report a systematic study of the ohmic contact scheme Ti/Al/Ti/Au, where the total film thickness was kept constant at 285 nm and the relative ratios of Ti/Al inner layer thicknesses were varied. While the film with the highest Ti/Al ratio had slightly inferior electrical properties, the layer smoothness and edge acuity were far superior to the other ohmic contact schemes.
 [DOI: 10.1149/1.2206998]

Manuscript submitted January 27, 2006; revised manuscript received March 20, 2006. Available electronically June 13, 2006.

AlGaN/GaN-based, high-electron mobility transistors (HEMTs) are very attractive for high-power, high-frequency devices due to the wide bandgap, high electron mobility, and high electron saturation velocity intrinsic to this materials system. Large ohmic contact resistance can lead to a serious deterioration of the peak current available from these devices. Several authors have studied the variation of the ohmic contact quality as a function of the composition of the ohmic contact. Ta/Ti/Al/Ni/Au,[1] Ti/Al/Mo/Au, Mo/Al/Mo/Au, V/Al/Mo/Au,[2] Ti/Al/Pd/Au,[3] and Ti/Al/Ti/Au[4] schemes have all been studied in the past several years.

Kim et al.[1] showed that low contact resistance (0.21 Ω mm) and good surface morphology could be obtained for Ta/Ti/Al/Au (10/30/120/400/500 nm) contacts. They attribute this good result to TaN/TiN interfacial layers, which they identify by synchrotron X-ray diffraction.

Selvanathan et al.[2] compared Ti/Al/Mo/Au, Mo/Al/Mo/Au, and V/Al/Mo/Au contact schemes. They found differences in the surface roughness, optimum anneal temperature, and long-term thermal stability between the three different contact schemes. Overall, they preferred the Ti/Al/Mo/Au scheme due to its combination of low contact resistance (0.38 Ω mm) and better thermal stability.

Fay et al.[3] studied the microstructure of Ti/Al/Pd/Au ohmic contacts using high-resolution transmission electron microscopy. They found that a relatively high anneal temperature of 950°C was required for the best ohmic contact resistance, which only went as low as 1.35 Ω mm. Moreover, the Pd layer did not prevent the diffusion of Au into the metal stack, with Au being found directly adjacent to the Ti-rich layer in all samples. In an older study,[4] the same group studied the Ti/Al/Ti/Au contact scheme, but was able to obtain a contact resistance of only 2.2 Ω mm. As this is the same contact scheme as is studied in the present work, it is useful to note that the layer thicknesses in Ref. 4 were 20/100/60/300 nm for Ti/Al/Ti/Au, respectively.

Gillespie et al.[5] studied four different metal stacks deposited on six different AlGaN/GaN epitaxial wafers from different suppliers. They found that different ohmic contact schemes were required to achieve the lowest possible contact resistance on each of the different wafers.

We have previously published a comparison between two ohmic contact schemes based on Ti/Al/Ti/Au.[6] We examined 20/100/45/55 nm and 30/80/120/55 nm film thicknesses, where the former was much richer in Al. The first contact scheme was found to have better contact resistance but much poorer surface morphology. The results suggested that an optimized scheme might be located at intermediate composition between the two schemes previously investigated. Thus, the aim of the present work was to optimize the Ti/Al/Ti/Au contact scheme by holding the total film thickness constant at 285 nm and varying the relative ratios of Ti/Al inner layer thicknesses.

Experimental

Table I shows the compositions of the ohmic contacts used in this work. In the first part of this work, the various contact schemes were applied to a single ammonia-molecular beam epitaxy (MBE) grown AlGaN/GaN HEMT structure, with undoped AlGaN thickness ~14 nm, mobility of 1130 cm^2/Vs, and carrier concentration of 1.62×10^{13} cm^{-2}. This particular wafer was grown as previously described.[7] It was cut using a diamond saw into eight equally sized, pie-shaped pieces. The pieces were then patterned with a Corbino contact resistance pattern, otherwise known as a circular transmission line pattern. Later in the paper, we also report on the annealing behavior of an assortment of other wafers during the ohmic contact step in a full HEMT process. These results are selected from our processing runs over the course of a year, and the AlGaN/GaN HEMT wafers had various structures and doping levels, but all had sheet resistance lower than 450 Ω/□. All were grown by ammonia-MBE, as described previously.[7]

In all cases, the metals were deposited by e-beam evaporation after the samples received a microwave descum and a 30 s dip in 1:1 HCl-H_2O. After lift-off, the samples were sequentially annealed in flowing N_2. Anneal temperatures ranged from 700 to 875°C. The wafers were coated on the back side with amorphous Si in order to improve heat transfer to the wafer in the rapid thermal annealing tools. Two different tools were used, an AG Associates Heatpulse 410, under thermocouple control and a Jipelec Jetfirst under pyrometer control. In both cases, the pieces were annealed face-up on a Si carrier wafer. The value of both the contact resistivity (r_c, Ω cm^2) and material sheet resistances (R_s, Ω/□) were measured using a four-probe method to eliminate the resistance of the leads. The contact resistance, R_c, in Ω mm is then given by $R_c = 10\sqrt{r_c R_s}$. In the process monitoring results, the resistance over a 5 μm Corbino gap was measured using a two-probe method, without removing the wa-

Table I. The thicknesses of the metal deposited for the different ohmic contact schemes used in this work. The 30 nm Ti layer is located adjacent to the AlGaN in the AlGaN/GaN layer structure.

Scheme	Ti (nm)	Al (nm)	Ti (nm)	Au (nm)	Ti/Al (mol/mol)
A	30	80	120	55	1.76
B	30	96	104	55	1.31
C	30	113	87	55	0.971
D	30	129	71	55	0.734
E	30	146	54	55	0.540
F	30	162	38	55	0.395

* Electrochemical Society Active Member.
z E-mail: jennifer.bardwell@nrc.ca

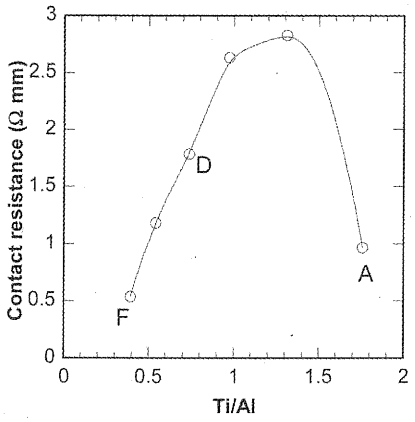

Figure 1. The contact resistance of the various contact schemes as a function of the Ti/Al molar ratio. The anneal temperature was 825°C. Samples A, D, and F are indicated for clarity.

fers from the cleanroom. After this brief test, the wafers could be immediately reannealed if necessary. Experience showed that samples with sheet resistance less than 450 Ω/□ and with a resistance of less than 30 Ω across the 5 μm gap would have contact resistance of approximately 1 Ω/mm when accurately measured using a four-point probe method.

The ohmic metal was examined in a Hitachi S-4700 field emission scanning electron microscope (FE-SEM) and by X-ray diffraction (XRD) using Philips 1729 X-ray generator at room temperature. Omega-2 theta scans were taken with a step size of 0.05° on patterned wafers. The values of 2θ, were offset so that the sapphire peak occurred at 41.68°.

Results and Discussion

The two schemes with the lowest contact resistances were Ti/Al/Ti/Au with layer thicknesses of 30/80/120/55 nm (scheme A) and 30/162/38/55 nm (scheme F), reaching contact resistances of 0.97 and 0.54 Ω mm, respectively, after an anneal temperature of 830°C. As shown in Fig. 1, the intermediate Ti/Al composition ratios showed much higher contact resistances.

This result was quite unexpected, because from the results of our previous study,[6] we hypothesized that a minimum contact resistance would be obtained when there was no excess metallic Al in the alloyed layer. According to the analysis in Ref. 6, scheme D would be expected to have the lowest contact resistance while maintaining good surface morphology. From Fig. 1, this is clearly not the case. However, the analysis in Ref. 6 was based on the assumption that one Au atom would substitute for one Al atom in the TiAl intermetallic compound. This was likely a naïve assumption, because all of the following intermetallic compounds are known to exist:[8] AlAu, Au_2Al, Au_3Al, and Au_2Ti. This indicates that many more possible intermetallic compounds are possible other than the single option we postulated.

The ohmic contacts were characterized by XRD, as shown in Fig. 2. The peaks were identified following the work of Kim et al.[1] They identified the phases TiN, AlTi, Al_2O_3, Al_2Au, AlNi, and Al_3Ti in their annealed Ti/Al/Ni/Au films, suggesting that it would be more appropriate to consider Au as a substitute for Ti (rather than for Al) in the intermetallic compounds present in the annealed film. For simplicity, only the diffraction patterns for the schemes with the two lowest (A and F) and the two highest (B and C) contact resistances were shown.

There are only small differences visible in these patterns. The most substantial difference is that sample F, which had the lowest contact resistance, contains the largest amount of Al_3Ti. This is likely because it contains the largest amount of Al. Sample A, which had the second lowest contact resistance, has the largest amount of

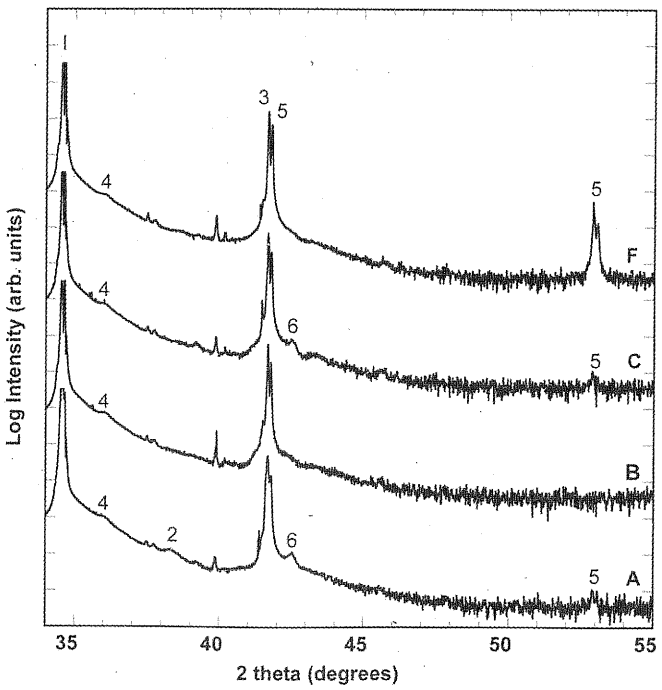

Figure 2. XRD patterns obtained from Ti/Al/Ti/Au contacts annealed at 830°C: (1) AlGaN/GaN, (2) AlTi, (3) Al_2O_3, (4) TiN, (5) Al_3Ti, and (6) Al_2Au.

AlTi. A small shoulder corresponding to TiN is visible in all samples. The peaks for the Al_2O_3 and Al_3Ti overlap strongly in the region of ~41.7°.

FE-SEM was used to characterize the film smoothness and edge acuity. While the film with the highest Ti/Al ratio (sample A) had slightly inferior electrical properties, the layer smoothness and edge acuity were far superior, as shown in Fig. 3. The film with the lowest Ti/Al ratio (sample F) had developed a very rough surface morphology and considerably deteriorated edge acuity after annealing. The surface morphology of the AlGaN/GaN surface in the center of the image is characteristic of the ammonia-MBE growth technique. It can be seen that the morphology of the semiconductor surface is carried through to the metal surface for scheme A, while for scheme F the roughness of the metallization scheme dominates the appearance of the surface. There was a continuous increase in metal roughness upon moving from scheme A to scheme F. The roughness is likely due to excess Al in the ohmic contact scheme, which does not form the intermetallic compounds AlTi and Al_3Ti, and thus is subject to melting at these high annealing temperatures.

The observed contact morphology strongly suggests that despite the slightly inferior contact resistance, scheme A is to be greatly preferred in practical applications, particularly when patterning very short gate lengths in a small opening close to the source electrode of the device. This scheme combines the potential of low contact resistance with superior surface morphology and edge acuity. Figure 4 shows an optical microscope image of a finished HEMT device. It is clear that the ohmic contact exhibits a smooth, specular surface, comparable in reflectivity to the gold of the gate pad. A nominal 0.5 μm long gate can easily be aligned within the gap between the smooth edges of the ohmic contact metals.

In our laboratory, we have used this scheme in fabricating numerous AlGaN/GaN devices over the past year. Many different AlGaN/GaN layer structures, such as doping of the AlGaN layer, addition of other layers such as a GaN cap, an AlN interlayer, etc., were fabricated. In almost all cases, excellent ohmic contacts with resistance less than 1 Ω mm were produced using this scheme. Figure 5 shows some selected results from the optimization of the anneal conditions for various wafers. However, each wafer required

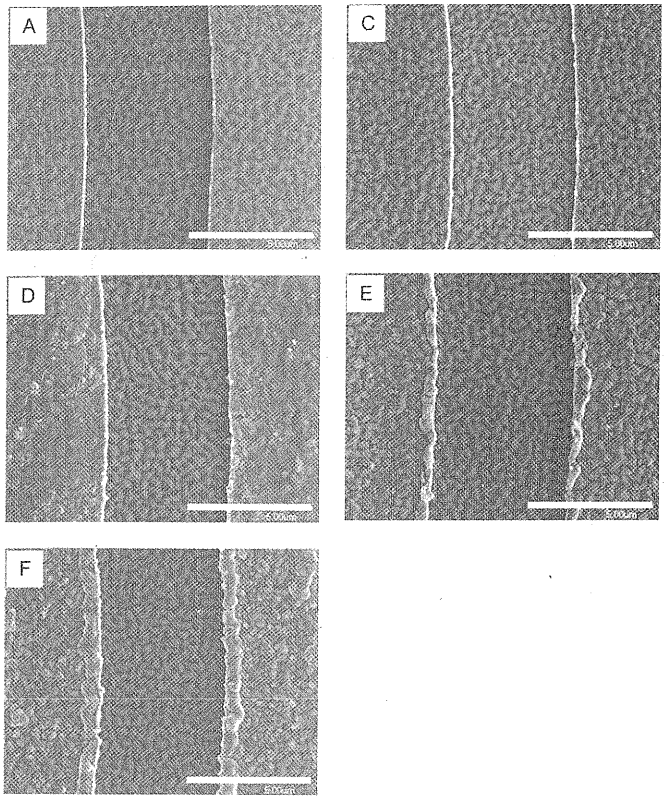

Figure 3. FE-SEM micrographs of different ohmic contact schemes. The images show the metal on either side of a 5 μm gap in the Corbino ring pattern. The bar indicates 5 μm.

individual attention to optimizing the anneal temperature. This is likely due to the variety of different growth structures that were used to produce this figure. In a production mode, standardized growth structures would be used, allowing the fabrication to be standardized with a single anneal recipe. Temperatures as low as 700 and as high as 845°C were required to obtain the desired contact resistance. Moreover, it is commonly observed that the contact resistance would initially increase before finally decreasing at sufficiently high anneal temperature. There is a large difference of about 100°C between the optimal temperature needed when the wafers were annealed under thermocouple control rather than under pyrometer control. Because two different annealing systems were used, the temperature calibration might vary slightly. However, by inserting a pyrometer in the normally thermocouple-controlled tool, we estimate that the thermocouple reads approximately 55°C less than the pyrometer at a temperature of 800°C. Thus, the different calibrations account for about half of this effect. In the case of pyrometer control, the initial starting anneal temperature was much higher than in the case of the thermocouple control, where a more extensive series of lower temperatures were initially used. Thus, the samples annealed under thermocouple control were exposed to much more total annealing time than those under pyrometer control. Thus, it seems likely that the additional difference in optimal anneal temperature is due to the more gradual and lengthy anneal conditions seen by the thermocouple control samples.

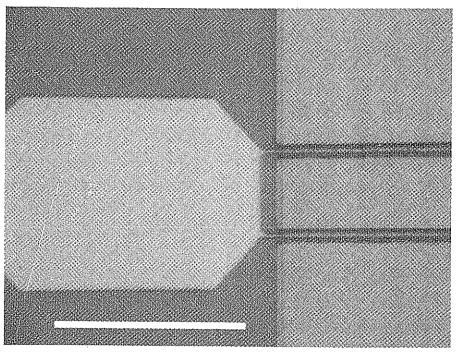

Figure 4. Optical microscopy of a finished device. The gold gate pad is located at the left of the image. The gate width is nominally 0.5 μm and was formed by contact lithography. The bar indicates 40 μm.

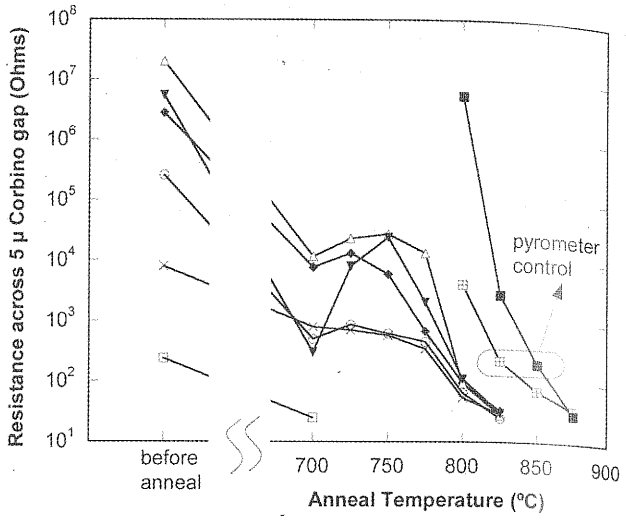

Figure 5. In cleanroom, two-point probe resistance measurements during the course of annealing various AlGaN/GaN HEMT device wafers. Most wafers were annealed under thermocouple control and the remainder (indicated) under pyrometer control.

The results of Fig. 5 confirm that ohmic contacts to AlGaN/GaN HEMTs do need a customized approach, as also noted by Gillespie et al.[5]

Conclusions

The contact scheme Ti/Al/Ti/Au, used for AlGaN/GaN HEMT ohmic contacts, was systematically studied. The film thickness of 285 nm was held constant, and the Ti/Al ratio of the two inner layers was varied. From the results of a previous study,[6] a minimum contact resistance at a Ti/Al (mol/mol) ratio of ~0.7 was expected. In contrast, the contact resistance showed a maximum at this value. Instead, the two schemes with the lowest contact resistances had Ti/Al ratios of 1.76 and 0.395, reaching contact resistances of 0.97 and 0.54 Ω mm, respectively, after an anneal temperature of 825°C. Despite the slightly higher contact resistance of the former scheme, the superior edge acuity and layer smoothness made it the contact scheme of choice for practical applications. Our experience with this contact scheme highlights the need for a customized approach to optimize the anneal temperature for different types of HEMT structures.

Acknowledgments

The authors are grateful for the skilled technical work of Jeff Fraser in collecting the FE-SEM images and Keyong Liu, Mark Malloy, and Hue Tran in the e-beam evaporation of the contacts.

The National Research Council, Canada, assisted in meeting the publication costs of this article.

References

1. K. H. Kim, C. M Jeon, S. H. Oh, J.-L. Lee, C. G. Park, J. H. Leè, K. S. Lee, and Y. M. Koo, *J. Vac. Sci. Technol. B*, **23**, 322 (2005).
2. D. Selvanathan, F. M. Mohammed, A. Tesfayesus, and I. Adesida, *J. Vac. Sci.*

Technol. B, **22**, 2409 (2004).
3. M. W. Fay, G. Moldovan, N. J. Weston, P. D. Brown, I. Harrison, K. P. Hilton, A. Masterton, D. Wallis, R. S. Balmer, M. J. Uren, and T. Martin, *J. Appl. Phys.*, **96**, 5588 (2004).
4. M. W. Fay, G. Moldovan, P. D. Brown, I. Harrison, J. C. Birbeck, B. T. Hughes, M. J. Uren, and T. Martin, *J. Appl. Phys.*, **92**, 94 (2002).
5. J. Gillespie, A. Crespo, R. Fitch, G. Jessen, and G. Via, *Solid-State Electron.*, **49**, 670 (2005).
6. J. A. Bardwell, G. I. Sproule, Y. Liu, H. Tang, J. B. Webb, J. Fraser, and P. Marshall, *J. Vac. Sci. Technol. B*, **20**, 1444 (2002).
7. S. Haffouz, H. Tang, J. A. Bardwell, E. M. Hsu, J. B. Webb, and S. Rolfe, *Solid-State Electron.*, **49**, 802 (2005).
8. O. Coreño-Alonso, *Intermetallics*, **14**, 475 (2006).